Impact of Liner Elasticity on Couple Stress Lubricated Partial Bearing

Sanjeev Kumar Lambha
Department of Mechanical Engineering National Institute of Technology, Kurukshetra

Kumar, Vinod
Department of Mechanical Engineering National Institute of Technology, Kurukshetra

Verma, Rajiv
Department of Mechanical Engineering National Institute of Technology, Kurukshetra

https://doi.org/10.5109/4774217

出版情報：Evergreen. 9 (1), pp.56-71, 2022-03. Transdisciplinary Research and Education Center for Green Technologies, Kyushu University
バージョン：

Impact of Liner Elasticity on Couple Stress Lubricated Partial Bearing

Sanjeev Kumar Lambha*, Vinod Kumar, Rajiv Verma
Department of Mechanical Engineering
National Institute of Technology, Kurukshetra
Kurukshetra, Haryana, India

*Author to whom correspondence should be addressed:
E-mail: sanjeev.lambha@gmail.com

(Received July 22, 2021; Revised November 28, 2021; accepted January 25, 2022).

Abstract: In this modern age of fast growing technology, it is required to attain the need of compact size and high speed of rotation in rotating machines. The lubrication is an important aspect along with the bearing geometry, which significantly influence the bearing conduct. The arc length studied here is 100 degrees for partial bearing with a medium for lubrication as fluid with couple stresses (i.e. *CSF*). The influence of elastic deformation along with the fluid on performance of bearing in static and dynamic manner is obtained by solving the modified Reynold's equation and an elasticity equation. The set of system equations are solved by using *FEM* approach. The results show a significant improvement in static and dynamic characteristics of partial bearing and the stability of the bearing is also improved while operating with couple stress fluid compared to Newtonian.

Keywords: EHL film lubrication, partial arc bearing, couple stress fluid, stability, static properties, dynamic properties

1. Introduction

The journal bearing with hydrodynamic lubrication are used from past decades as an important application in rotating machines. It is required to understand the correct geometry to attain the emerging increased need of high rotational speed with machine compactness as well as high load carrying capacity in modern machineries. From geometry point of view, the bearings are used according to the arc length, which covers the shaft (journal). The bearing with arc length of 360° are most preferably used which are known as full journal bearings but the bearings with arc length less than 360° known as partial bearing. Partial bearings have their remarkable influence on the performance of rotating system over full journal bearing, in cases of small-scale applications with high speeds. The partial journal bearings are characterized as their notable advantage compared to the full bearing systems. In case of high speed rotating machines, the introduction of vibrations and unbalanced forces causes the system to be failure. So to get the exact solution of performance characteristics, the effect of elasticity of journal and bearing both should also be considered practically while analysis. An assumption is made that the journal is a rigid body whereas the bearing is an elastic body because the material used for journal is more inflexible than material of bearing. The effect of elastic deformation on the conduct of bearings with partial arc is also required to be studied. In the series of determination of significant effects of various parameters on the conduct of bearing with partial arc, the results were in good agreement with the available results of Raimondi when compared for statically and dynamically rather numerically[1)]. A study was performed[2)] to know the effect of change in arc length as 150° on the force unbalanced and its transmission in a system of bearing with symmetric rotor. The Reynold's equation for partial arc gas bearing was solved by an inexpensive, fast and accurate approach[3)] using Galerkin's method. The bearing load and stability derivatives were obtained by solving the set of equations in standard form according to compressibility number. The results for a journal bearing having an arc length of 60° with the consideration of two values of clearance ratios and Reynolds number up to 12000 emulated[4)] with the turbulent theory available and the laminar theory as well. A good resemblance for some particular range of empirical factor was observed whereas the correlation becomes poorer progressively beyond this range. The bearing of arc length 120° studied[5)] to find the effects of variation in compressibility factor ranging 0 to infinite, which showed that at low compressibility numbers the bearing clearance ratio and pivot location maintained close to the optimum conditions for highest load capacity

and minimum frictional coefficient. It was founded that the bearing load capacity and coefficient of friction effected substantially due to choice of pivot location for higher compressibility numbers. The magneto hydrodynamic partial bearing studied analytically and experimentally[6] such that the external current flow axially between journal and bearing by an induced external field. The experimental results showed an optimum Hartman number to give an increased load carrying capacity peaks and have good agreement with theory. The study of steady state and dynamic characteristics for the two geometries of self-acting journal bearings (360° arc and 100° arc)[7] in super laminar regimes up to the range of mean Reynolds number 13300 showed that test performed were in good agreement with that of the data available in published theory. It was also concluded that theory generated may be used to design various bearings working on the principle of self-acting in high speed machinery and a lubrication of fluid with low kinematic viscosity, either in laminar or in super laminar flow regimes. An approximate numerical method used to solve the equations of a 100° arc partial bearing[8]. It was concluded that while considering the isothermal solution with the dependence on bearing angle and aspect ratio; the thermo-hydrodynamic effect lessens the dependence of specific load on constant eccentricity. The effect of deformation coefficient on a bearing arc of short span (60°) is more compared to a long span (120°) whereas there was a reduction in attitude angle for 60° and 120° type bearing span with an increase in deformation[9]. The design chart of various parameters was presented[10] for conduct of centrally loaded gas bearings with partial arc. The rotationally non-symmetric bearings i.e. pivoted pad radial bearings, bearings with partial arc, and oil grooved pivoted bearings modelled by a method[11] of mobility and impedence tensor introduced for modelling of journal bearings. It was observed that the capacity of load carrying decreased for an increase in the misalignment factor and increase in non-Newtonian behaviour[12], while studying the influence of misalignment in bearings with partial arc. The thermo-hydrodynamic solution of a finite width partial arc bearing lubricated by non-Newtonian lubricants was obtained[13] with an assumption, that the flow of heat was observed in radial direction only, in respect of the bush. The static characteristics were compared with the experimental results by using an approximate solution method[14] which shows a good agreement. The impact of heat transfers on surfaces of journal and bearing bush also analysed by assuming the adiabatic boundary conditions. The combined effect of pad deformation and mixed lubrication studied by using a deterministic numerical solution[15] for partial journal bearing. The impact of circumferential scratches studied[16] on the conduct of partial bearing in continuation of previous research. The impact of change in bearing eccentricity, arc angle, slenderness ratio and the dimple shape, showed an effective improvement in bearing performances compared to smooth bearings[17] in terms of friction coefficient. The resilience in liner had a significant influence on the conduct of cylindrical bearing[18]. A combined approach with the combination of FEM and a new method known as boundary element used[19] to analyse the deformation in bearing housing. The conduct of journal bearing with an impact of flexibility in liner, determined[20] by deformation coefficient parameter defined relatively by the factors R_j, C, t, μ, U_o and E_m. An inverse model of porous bearing with flexibility was proposed[21] to evaluate the parameter of permeability and eccentric ratio. In case of diesel engines, the journal bearings are widely used so it is required to know performance of system with bearings. In this concern, the dimensions of bearings and stiffness in housing combined on connecting rod was studied[22]. A numerical algorithm through which the Reylond's: Koiter model solved for differentiating the effect of elasticity on load constraint presented[23] to predict the distribution of pressure in fluid film properly.

Conventionally it was assumed that behaviour of lubricant to be Newtonian for elasto-hydrodynamic lubrication. Whereas on going through the extensive literature review it was founded that to fulfil the emerging demands of modern machineries, the performance of lubricant need to be upgraded. In this view the performance of lubricant is going to be changed and improved when the additives are added with them such that the lubricant becomes Newtonian to non-Newtonian. The influence of the types and viscosities of lubricants on the basis of interaction with refrigerant, effect on compressor and impact on system performance were investigated[24] which for developing new lubricants to be used in heat pump for better efficiency. The rheology of the working fluid as non-Newtonian[25] examined to investigate the particles effect for spiral and circular pipes. When the Newtonian fluids are blended with polymer additives of long chain, the nature of fluid becomes non-Newtonian and it is known to be a *CSF* (Couple Stress Fluid). The rheological behaviour of non-Newtonian lubricants was explained by many micro-continuum theories. The influence of couple stresses was elaborated on the basis of small micro-continuum theory, by a model known as Stokes model[26]. The load capacity improvised and the friction coefficient reduced on addition of polymer particles to lubricants[27-28]. The properties because of an action of squeezing in bearings with partial arc studied by a model[29-31] for a lubrication of (*CSF*). The impact of liner flexibility with (*CSP*) studied[32] and concluded that with an improvement in static and dynamic properties, the load capacity of cylindrical journal bearing also enhanced. The key factors, which govern the highest load capacity and film thickness ratio, were bearing geometric features, factor of couple stress and magnetic based parameters[33]. The impact of *CSP* on the conduct of double layered bearing showed[34] that load capacity increased whereas friction reduced. The wear and friction near edges were

decreased[35] by using the (*CSF*) in finite line contacts. A 3-D elasticity model[36] was used for *CSP* and elasticity parameter to evaluate the static and dynamic performance characteristics along with stability parameters for hydrodynamic journal bearing. On evaluating the static and dynamic characteristics of circular bearing[37], it was founded that the non-linear trajectories become unstable for the condition of equivalence in mass with critical mass for both Newtonian and micropolar fluid. The impacts of irregularities in shapes for a six pocket bearings[38] indicated that the bearing performance was influenced due to presence of geometrical irregularities, whereas the characteristic parameters have an improvement by using fluid with couple stress as lubricant. The amount of radial deformation had different values in both the upper as well as lower lobe in two lobe bearing[39] for different couple stress parameter and eccentricity ratio. The stiffness and damping coefficients as dynamic characteristics with static properties were obtained for different values of couple stress parameter[43], which showed a significant improvement in dynamic coefficients of bearing. A flexible journal bearing lubricated with non-Newtonian nanolubricant studied and compared with rigid bearings to find the static performance for different values of power law index and eccentricity ratio[44]. The maximum pressure, load capacity and friction force or nanolubricants increased compared to base lubricant whereas decreased for all values of power law index due to elastic deformation. The introduction of couple stresses in fluids improved the efficiency of two lobe bearings[45] showed an increase in load capacity, reduction in attitude angle and enhanced the damp ability of bearings to rotor perturbations which in turn improvise the stability. In a combined study[46] of turbulence and non-Newtonian lubrication the static, dynamic and stability characteristics showed an enhancement in performance of the bearings.

Through an extensive literature review as mentioned above it is obvious that the impact of elasticity in bearing liner and (*CSF*) is significant and is required to evaluate the performance characteristics with these parameters. This paper includes the study of properties in a bearing with partial arc in terms of static and dynamic behaviour. The cumulative effect of deformation in bearing and (*CSP*) is evaluated in this paper. The approach used for solution of system equations is *FEM* (i.e. *Finite Element Method*). A *100°* arc of bearing considered with $\lambda = 1.0$ for analysis to know the effect using a bearing of arc length between long arc (180- degree) and short arc (60-degree). The properties discussed are capacity of load bearing, pressure distributed, stability parameters and other performance characteristics of static behaviour and dynamic behaviour. The study of partial arc bearing using couple stress fluid with bearing flexibility has not been studied yet to the best knowledge of authors. This study will be helpful for the designers and researchers for enhancement in performance of bearing with partial arcs.

2. Analysis

A system of bearing with partial arc with a bearing arc of *100°*, denoted by β and a flexible liner of thickness t considered here in this study for analysis. The bearing with its geometric properties for partial arc is represented by Fig. 1 in which the journal is characterized by radius R_j with O_j as the center of journal and the bearing center is depicted as O_b with R_b as the radius of bearing. The gap between the journal and liner surfaces separated with fluid film, known as clearance space and denoted by c, such that the fluid used is non-Newtonian in nature. The fluid used for lubrication, blended with the polymer additives of long chain to the fluid of Newtonian nature, considering the polar effects, which is termed as the (*CSF*). The body forces and body couples are assumed to be absent during the analysis. The characteristics of couple stress fluid are defined by the characteristic length (l) of couple stress fluid, where $l = (\eta/\mu)^{1/2}$ which depends on new material constant denoted by η, such that $l^* = l/c$ (non-dimensional). The Reynold's equation in general terms for fluid flow alongwith the elasticity equation for deformation in bearing liner are solved simultaneously to calculate the performance of a journal bearing system. The set of equations used for the formulation of system explained below.

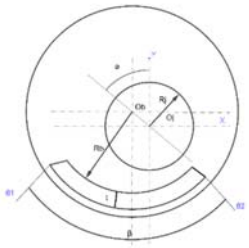

Fig. 1: Geometry of bearing with partial arc with flexible liner

2.1. Modified Reynold's equation

The flow of fluid between the journal and liner surfaces alongwith flexibility is commanded by the modified Reynold's equation. The governing (Reynold's) equation[40] of the couple stress fluid flow obtained by using the continuity equation and momentum equation based on the stokes model[26] assuming the lubrication theory of thin film for an incompressible flow. The continuity equation and the momentum equation governing the motion are:

$$\rho \frac{Dv}{Dt} = -\nabla p + \rho \boldsymbol{F} + {}^{1}/_{2}\,\rho \nabla \mathrm{x}\mathbf{C} + \mu\nabla^2 - \eta\nabla^4 \boldsymbol{V} \tag{1}$$

$$\nabla V = 0 \tag{2}$$

where, $\boldsymbol{V}$ = *Velocity vector,*

$\boldsymbol{F}$ = *Body force per unit mass,*

C = *Body couple per unit mass,*

ρ = *Density,*

μ = *shear viscosity,*

p = *pressure,*

η = *material constant responsible for couple stress fluid property.*

After applying the assumptions made for the study, motion equation in Cartesian coordinate can be expressed as:

$$\frac{\partial p}{\partial x} = \mu\frac{\partial^2 u}{\partial y^2} - \eta\frac{\partial^4 u}{\partial y^4} \quad (3)$$

$$\frac{\partial p}{\partial y} = 0 \quad (4)$$

$$\frac{\partial p}{\partial z} = \mu\frac{\partial^2 w}{\partial y^2} - \eta\frac{\partial^4 w}{\partial y^4} \quad (5)$$

$$\frac{\partial u}{\partial x} + \frac{\partial v}{\partial y} + \frac{\partial w}{\partial z} = 0 \quad (6)$$

u, v, w denotes the velocity components in x, y, z directions.

The boundary conditions applicable to bearing as well as journal surface are:

$$u_{y=0} = 0;\ v_{y=0} = 0;\ w_{y=0} = 0 \quad (7.1)$$

$$\frac{\partial^2 u}{\partial y^2}_{y=0} = \frac{\partial^2 w}{\partial y^2}_{y=0} = 0 \quad (7.2)$$

(equation (7) for bearing surface)

$$u_{y=h} = U;\ v_{y=h} = V;\ w_{y=h} = 0 \quad (8.1)$$

$$\frac{\partial^2 u}{\partial y^2}_{y=h} = \frac{\partial^2 w}{\partial y^2}_{y=h} = 0 \quad (8.2)$$

Integrating equation (3) and equation (5) by applying boundary conditions to get velocity components as:

$$u = U\,{}^{y}\!/_{h} + {}^{1}\!/_{2\mu}\frac{\partial p}{\partial x}\left\{y(y-h) + 2l^2\left(1 - \frac{\cos h\left(\frac{2y-h}{2l}\right)}{\cos h\left({}^{h}\!/_{2l}\right)}\right)\right\} \quad (9.1)$$

$$w = \frac{1}{2\mu}\frac{\partial p}{\partial z}\left\{y(y-h) + 2l^2\left(1 - \frac{\cos h\left(\frac{2y-h}{2l}\right)}{\cos h\left({}^{h}\!/_{2l}\right)}\right)\right\} \quad (9.2)$$

where, $l = \sqrt{{}^{\eta}\!/_{\mu}}$, characteristic length of additives

The modified form of Reynolds equation can be obtained by integrating the continuity equation (6) w.r.t. y using velocity components with the boundary condition as below:

$$\frac{\partial}{\partial x}\left(G(h,l)\frac{\partial p}{\partial x}\right) + \frac{\partial}{\partial z}\left(G(h,l)\frac{\partial p}{\partial z}\right) = 6\mu\left(U\frac{\partial h}{\partial x} + 2V\right) \quad (10)$$

In non-dimensional form the flow equation can be expressed as,

$$\frac{\partial}{\partial\theta}\left(\frac{G(\bar{h},l^*)}{\bar{\mu}}\frac{\partial\bar{p}}{\partial\theta}\right) + \frac{1}{4\lambda^2}\frac{\partial}{\partial\bar{Z}}\left(\frac{G(\bar{h},l^*)}{\bar{\mu}}\frac{\partial\bar{p}}{\partial\bar{Z}}\right) = 6\frac{\partial\bar{h}}{\partial\theta} + 12\frac{\partial\bar{h}}{\partial\tau} \quad (11)$$

where, $G\left(\bar{h},l^*\right) = \bar{h}^3 - 12l^{*2}\bar{h} + 24l^{*3}\tan h\left(\frac{\bar{h}}{2l^*}\right)$

The factors used for non-dimensionalisation of equation (1) are,

$$\theta = \frac{X}{R_j};\ \bar{Z} = \frac{Z}{L};\lambda = \frac{L}{2R_j};\ \bar{h} = \frac{h}{c};\ h = 1 + \varepsilon\cos\theta;\ \varepsilon = \frac{e}{c};$$

$$\bar{p} = \frac{pc^2}{\mu_0\omega_j R_j^2};\ \bar{\mu} = \frac{\mu}{\mu_0};\ \tau = \omega_j t;\ U = R_j\omega_j;$$
$$l^* = {}^{l}\!/_{c};\ l = \sqrt{{}^{\eta}\!/_{\mu}}$$

η = new material constant, such that η = 0 for Newtonian fluids, and

μ = Newtonian viscosity (Dynamic viscosity).

The expression for thickness of fluid film for the journal bearing system with liner flexibility is expressed by;

$$\bar{h} = 1 - \left(\bar{X}_j - \Delta\bar{X}\right)\cos\theta - \left(\bar{Z}_j - \Delta\bar{Z}\right)\sin\theta + \bar{\delta}_r \quad (12)$$

where, $\bar{X}j$ & $\bar{Z}j$ = the steady state coordinates of journal center

such that $\bar{X}j = \varepsilon\sin\phi$, & $\bar{Z}j = -\varepsilon\cos\phi$,

$\Delta\bar{X}$ *and* $\Delta\bar{Z}$ = the perturbation components of journal center from steady state,

$\bar{\delta}_r$ = the radial deformation of bearing liner

2.2. FEM formulation of Reynolds equation

The equation of fluid flow *Eq. (11)* is a nonlinear differential equation, which have a complex form of solution, and it is complicated to solve the equation analytically, so an approach of *Finite Element Method* introduced here for the solution the equations. The fluid flow is discretized into elements with The variation of pressure $\bar{p}$ over an element *e* in the discretized flow field is represented by:

$$\bar{p}^e = \sum_{i=1}^{i=4} N_i \bar{p}_i^e \ ; \quad (13)$$

where,

N_i = shape function for the i^{th} node, &

$\bar{p}_i^e$ = corresponding nodal pressure of e^{th} element

Now after applying the Galerkin's orthogonal residual approach for the solution of equation (11), the form of equation after finite element formulation can be expressed as:

$$\sum_{i=1}^{i=n} \iint \left[\frac{\partial}{\partial\theta}\left(\frac{G(\bar{h},l^*)}{\mu}\frac{\partial p^e}{\partial\theta}\right) + \frac{\partial 1}{4\lambda^2}\frac{\partial}{\partial\bar{Z}}\left(\frac{G(\bar{h},l^*)}{\mu}\frac{\partial p^e}{\partial\bar{Z}}\right) - 6\frac{\partial\bar{h}}{\partial\theta} - 12\frac{\partial\bar{h}}{\partial\tau}\right] N_i^e \, d\theta \, d\bar{Z} = 0 \quad (14)$$

It can also be written as

$$\sum_{i=1}^{i=n}\left([F_{ij}^e][\bar{p}_i^e] - [A_{ij}^e] - [B_i^e]\right) = 0 \quad (15)$$

For isoviscous lubricants, μ = 1.0 (here the viscosity is independent of both the pressure and temperature)

From equation (15);

$$[F_{ij}^e] = \iint_{A^e}\left\{G(\bar{h},l^*)\left[\frac{\partial N_i^e}{\partial\theta}\frac{\partial N_j^e}{\partial\theta} + \frac{\partial N_i^e}{\partial\bar{Z}}\frac{\partial N_j^e}{\partial\bar{Z}}\right]\right\} d\theta d\bar{Z} \quad , \quad (16.1)$$

i, j = 1,2,3,4

$$[A_{ij}^e] = 6\iint_{A^e}\frac{\partial\bar{h}}{\partial\theta}N_i^e \, d\theta d\bar{Z}, \quad i, j = 1,2,3,4 \quad (16.2)$$

$$[B_i^e] = 12\iint_{A^e}\frac{\partial\bar{h}}{\partial\tau}N_i^e \ d\theta d\bar{Z} = 0, \ i, j = 1,2,3,4 \quad (16.3)$$

The expression for complete domain of fluid flow is expressed as:

$$[F_{ij}][\bar{p}_i] = [A_{ij}] \quad (17)$$

where,

$[F_{ij}]$ = Assembled coefficient matrix also known as *fluidity matrix*,

$[A_{ij}]$ = Assembled column vector consisting of vector terms,

$[\bar{p}_i]$ = Nodal pressure vector.

The pressure distribution for a system of bearing with partial arc and flexible liner is obtained by solving the equation (14) along with an elasticity equation (18) used to find the impact of deformation in liner used in bearing, as discussed in section below.

2.3. Deformation of Bearing Liner

As the liner is flexible compared to the journal and the bearing housing material, the deformation in the liner effects the conduct of the system considerably. The approach used to discretize the bearing liner is an isoparametric, 8-noded hexahedral elements as shown in Fig. 2. The displacement of any node in the liner is in three directions viz. circumferential, radial and axial as δ_x, δ_y, δ_z. For calculation of deformation in liner due to film thickness, only radial (δ_y) component is considered as the effect of tangential force is negligible on the circumferential deformations for the present analysis.

The displacement in three direction is represented by,

$\delta = \begin{Bmatrix}\delta x\\ \delta y\\ \delta z\end{Bmatrix}$, and for this study the expression used for deformation is $\delta_r = \begin{Bmatrix}0\\ \delta y\\ 0\end{Bmatrix}$ as only radial deformation is considered for effect of flexibility in partial bearing. The deformation of liner in radial direction is obtained by using an elasticity equation[36] for the discretized bearing liner, expressed as:

$$[\bar{K}]\{\bar{\delta}_r\} = C_d\{\bar{F}\} \quad (18)$$

where,

$[\bar{K}] = \left(1/_{E_L R_j}\right)[K]$ *(known as stiffness matrix)* $\left(\because [K]^e = \int_V \bar{B}^T\bar{D}\bar{B}dV^e\right)$ (19.1)

$\{\bar{F}\} = \left(c^2/_{\bar{p}\mu_0\omega_j R_j^4}\right)\{F\}$ *(surface traction vector)* $\because \left(\{F\}^e = \int_{A^e} N^T F dA^e\right)$ (19.2)

$\{\bar{\delta}_r\} = \left(\frac{1}{c}\right)\{\delta_r\}$ *(displacement vector)* $\left(\because \{\delta_r\} = (C_d \times \bar{p})\right)$ (19.3)

$C_d = \left(\frac{\mu_0\omega_j}{E}\right)\left(\frac{t\bar{h}}{R_j}\right)\left(\frac{R_j^3}{c^3}\right)$ *(coefficient of deformation)* (19.4)

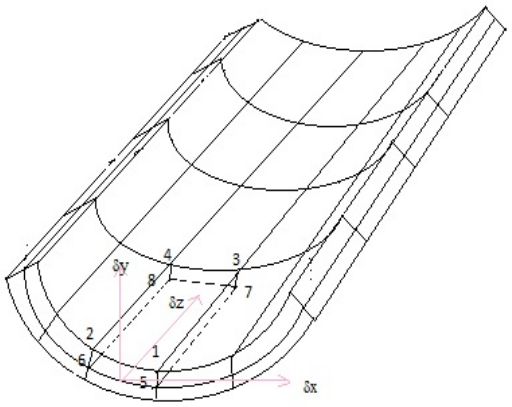

Fig. 2: Eight-noded hexahedral discretised liner

2.4. Performance Characteristics

The pressure obtained from the iterative solution of Reynold's equation along with elasticity equation is used to calculate the various characteristics of bearing with partial arc system. The behavior of the system is represented by static characteristics and dynamic characteristics.

The characteristics of the system statically calculated in this analysis are as follows:

Load Bearing Capacity:

The capacity of load bearing has its two components for journal bearing. The load capacity of the system can be calculated by using the expressions[20] of radial and tangential components as expressed below:

$$\bar{W}_x = \int_{\beta_1}^{\beta_2}\int_{-1}^{+1} \bar{p}\cos\theta \, d\theta d\bar{z} \quad \text{and}$$

$$\bar{W}_z = \int_{\beta_1}^{\beta_2}\int_{-1}^{+1} \bar{p}\sin\theta \, d\theta d\bar{z} \tag{20}$$

The expression for obtaining the load capacity is as follows:

$$\bar{W} = \sqrt{\bar{W}_x^2 + \bar{W}_z^2} \tag{21}$$

The attitude angle can also be obtained by using equation (12) as follows:

$$\tan\emptyset = \frac{\bar{W}_z}{\bar{W}_x} \tag{22}$$

The Somerfield number can be expressed as:

$$S = \frac{2\lambda}{\pi\bar{W}} \tag{23}$$

The static characteristics obtained at the position of steady state of journal, whereas the characteristics obtained at disturbed position of journal are dynamic characteristics. These dynamic properties give a measure to the stability of the system of journal bearing at the position of disturbed system. The dynamic response for the system of journal bearing is calculated by obtaining the associated stiffness and damping properties. The expressions used for calculation of stiffness characteristics are as follows:

$$\begin{bmatrix}\bar{K}_{xx} & \bar{K}_{xz}\\ \bar{K}_{zx} & \bar{K}_{zz}\end{bmatrix} = \begin{bmatrix}\frac{d}{d\bar{X}}\\ \frac{d}{d\bar{Z}}\end{bmatrix}[\bar{W}_x \quad \bar{W}_z] \tag{24.1}$$

(*where,* $\dot{\bar{X}} = \dot{\bar{Z}} = 0$)

$$\begin{bmatrix}\bar{K}_{xx} & \bar{K}_{xz}\\ \bar{K}_{zx} & \bar{K}_{zz}\end{bmatrix} = -\int_{\beta_1}^{\beta_2}\int_{-1}^{+1}\begin{bmatrix}\frac{d\bar{p}}{d\bar{X}}\\ \frac{d\bar{p}}{d\bar{Z}}\end{bmatrix}[\cos\theta \quad \sin\theta]d\theta d\bar{Z} \tag{24.2}$$

Whereas the expressions for calculation of damping characteristics are:

$$\begin{bmatrix}\bar{C}_{xx} & \bar{C}_{xz}\\ \bar{C}_{zx} & \bar{C}_{zz}\end{bmatrix} = -\begin{bmatrix}\frac{d}{d\bar{X}}\\ \frac{d}{d\bar{Z}}\end{bmatrix}[\bar{W}_x \quad \bar{W}_z] \tag{25.1}$$

(*where,* $\dot{\bar{X}} = \dot{\bar{Z}} = 0$)

$$\begin{bmatrix}\bar{C}_{xx} & \bar{C}_{xz}\\ \bar{C}_{zx} & \bar{C}_{zz}\end{bmatrix} = -\int_{\beta_1}^{\beta_2}\int_{-1}^{+1}\begin{bmatrix}\frac{d\bar{p}}{d\dot{\bar{X}}}\\ \frac{d\bar{p}}{d\dot{\bar{Z}}}\end{bmatrix}[\cos\theta \quad \sin\theta]d\theta d\bar{Z} \tag{25.2}$$

The values of $\frac{d\bar{p}}{d\bar{X}}, \frac{d\bar{p}}{d\bar{Z}}, \frac{d\bar{p}}{d\dot{\bar{X}}}, \frac{d\bar{p}}{d\dot{\bar{Z}}}$ are obtained by solving the Reynolds's equation expressed above.

The non-dimensional form of linearized motion equations is:

$$[\bar{M}_j]\left[\ddot{\bar{X}}\right] = [\bar{C}_{ij}]\left[\dot{\bar{X}}\right] + [\bar{K}_{ij}][\bar{X}] \tag{26.1}$$

$$[\bar{M}_j]\left[\ddot{\bar{Z}}\right] = [\bar{C}_{ij}]\left[\dot{\bar{Z}}\right] + [\bar{K}_{ij}][\bar{Z}] \tag{26.2}$$

Thus, equation for distributed motion of journal can be expressed as:

$$[\bar{M}_j]\begin{bmatrix}\ddot{\bar{X}}\\ \ddot{\bar{Z}}\end{bmatrix} = \begin{Bmatrix}\Delta F_X(\bar{X},\bar{Z},\dot{\bar{X}},\dot{\bar{Z}})\\ \Delta F_Z(\bar{X},\bar{Z},\dot{\bar{X}},\dot{\bar{Z}})\end{Bmatrix} \tag{27}$$

where, $[\bar{M}_j] = \begin{bmatrix}\bar{M}_j & 0\\ 0 & \bar{M}_j\end{bmatrix}$ = ($\bar{M}_j$ is the diagonal mass matrix),

$\begin{bmatrix}\ddot{\bar{X}}\\ \ddot{\bar{Z}}\end{bmatrix}$ = the components of acceleration in *X* and *Z* directions,

ΔF_X and ΔF_Z = unbalance forces on journal in *X* and *Z* directions.

By substituting the respective values, the equation of motion can be expressed as:

$$\bar{M}_j\ddot{X} - \bar{C}_{XX}\dot{\bar{X}} - \bar{C}_{XZ}\dot{\bar{Z}} - \bar{K}_{XX}\bar{X} - \bar{K}_{XZ}\bar{Z} = 0 \tag{28.1}$$

$$\bar{M}_j\ddot{Z} - \bar{C}_{ZX}\dot{\bar{X}} - \bar{C}_{ZZ}\dot{\bar{Z}} - \bar{K}_{XZ}\bar{X} - \bar{K}_{ZZ}\bar{Z} = 0 \tag{28.2}$$

The characteristic equation in form of polynomial equation can be written as:

$$\sigma^4 + A_1\sigma^3 + A_2\sigma^2 + A_3\sigma + A_4 = 0 \tag{29}$$

where, σ = *Complex variable,*

A_i = *function for mass of journal & dynamic coefficients.* *i = 1, 2, 3…….*

The polynomial form of characteristic equation is solved by using the Routh's criteria to know the stability in a system of the bearing with partial arc, in terms of critical mass ($\bar{M}_c$). For a stable system it is assumed that the value of $\bar{M}_j$ should be less than $\bar{M}_c$.

Threshold speed (the speed of journal at instability

threshold) is calculated by the use of expression as expressed below:

$$\omega_{th} = \sqrt{\frac{\bar{M}_c}{\bar{W}}} \tag{30}$$

where, $\bar{M}_c = {KI}/{\nu^2}$

$$\nu^2 = \frac{(\bar{K}_{XX}-KI)(\bar{K}_{ZZ}-KI)-\bar{K}_{XZ}\bar{K}_{ZX}}{(\bar{C}_{XX}\bar{C}_{ZZ}-\bar{C}_{XZ}\bar{C}_{ZX})}, \tag{31}$$

(υ is the whirl frequency ratio at threshold instability)

$$KI = \frac{(\bar{K}_{XX}\bar{C}_{ZZ}+\bar{K}_{ZZ}\bar{C}_{XX}-\bar{K}_{XZ}\bar{C}_{ZX}-\bar{K}_{ZX}\bar{C}_{XZ})}{(\bar{C}_{XX}+\bar{C}_{ZZ})} \tag{32}$$

2.5. Solution Procedure

The set of equations used in the present study, solved by applying an iterative scheme/procedure to find the nodal pressure in first stage of solution. The input parameters are initialised primarily at an initial stage. The system initialized by storing some initial values of ε and ϕ along with the other required geometric properties into the memory of the program.

The elastic deformation of liner changes the film thickness under various loading conditions for bearing with partial arc. Due to this change in film thickness the pressure at different node positions also changes because of the deformation in liner. The sketch of the solution procedure is shown in Fig. 3.

Thus with consideration of initial values stored in first step the nodal pressures at various node positions are calculated, by the solution of Reynolds equation (equation (4)) along with the equation of elasticity as equation (8). The solution of the equations is obtained by using Gauss Siedel iterative approach such that it should satisfy the boundary conditions stated as follows:

$$\bar{p} = 0 \;\; at \;\; \bar{z} = \; -1 \tag{33.1}$$

$$\bar{p} = 0 \;\; at \;\; \bar{z} = \; +1 \tag{33.2}$$

$$\bar{p} = 0 \;\; at \;\; \bar{z} = \; \beta_1 \tag{33.3}$$

$$\bar{p} = 0 \;\; at \;\; \bar{z} = \; \beta_2 \tag{33.4}$$

$$\left(\frac{\partial \bar{p}}{\partial \alpha}\right)_{\alpha_2} = 0, \textit{ Trailing edge} \tag{33.5}$$

$$\left(\frac{P_i^k - P_{i-1}^k}{P_i^k}\right) < (1/10^5), \textit{ pressure convergence criteria} \tag{33.6}$$

where, i is iteration index and k = 1,2, 3….. n.

The thickness of fluid film obtained once are used to find the pressure distributed along the film thickness, which satisfy the boundary conditions mentioned above. The same procedure is continued in a repetitive way for the ε = 0.1, 0.3, 0.5 and (l^*) as 0.0, 0.1, 0.2.

3. Results and Discussions

In elasto-hydrodynamic lubrication analysis, the material for liner is softer than the material used for journal and bearing housing. Therefore, due to difference in pressure profile at the interaction of surfaces, a deformation in liner is produced. As in fluid film the pressure is a function of the factors μ_o, ω, R_j, and c, so with the deformation of bearing liner the fluid film thickness varies due which the pressure distribution also varies. So it is obvious that the deformation of liner and the distribution of pressure are two interdependent properties. The property of the fluid used for lubrication have an impact on the fluid film thickness. According to stokes theory of micro continuum, on adding some additives to

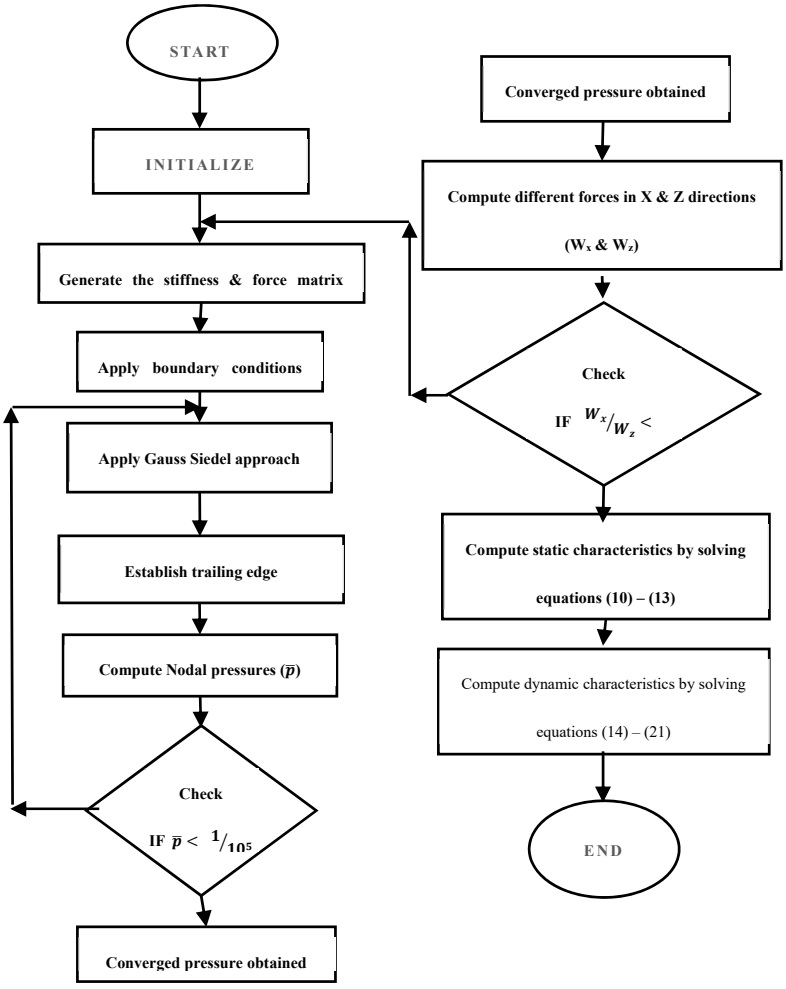

Fig. 3: Solution Procedure

the fluid of Newtonian nature the molecular dimension of fluid changes. The factor η is responsible for the property of couple stresses in lubricants of Non-Newtonian nature. (*CSF*) is characterizes by the characteristic length, $l = (\eta/\mu)^{1/2}$, whereas the factor $l^* = l/c$ termed as the parameter for couple stresses (*CSP*) which characterizes the effect of couple stress on the system. A cumulative effect of (C_d) and (*CSP*) studied here to determine the performance characteristics

(statically and dynamically) of a 100° arc journal bearing. The properties of the system are obtained statically and dynamically for (*CSP*), (*l**) as 0.0 (rigid), 0.1, and 0.2, whereas the (C_d) varies from 0.0 to 1.0.

To check the affirmation of model and solution procedure used to obtain results in this study, the results for circular journal bearing and 120° are compared and validated with the published results in form of plots and table below.

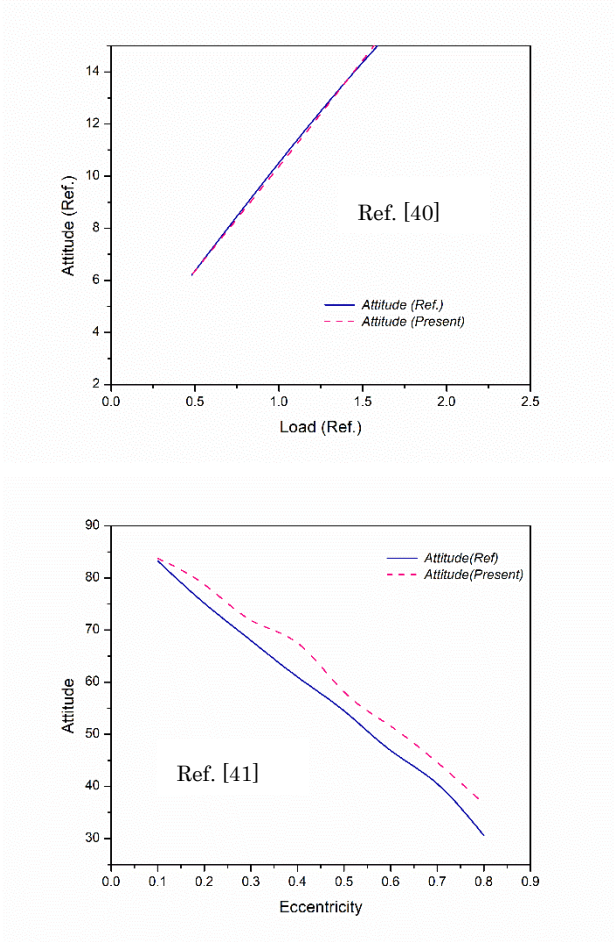

Fig. 4: Validation of static properties

The static characteristics are validated by comparing the results of circular bearing for variation of attitude angle with load carrying [40] and eccentricity ratio [41] both in Fig. 4. The program is validated to use for study of partial bearing by comparing the results of 120^0 partial arc journal bearing in Table After going through an extensive literature review, it is observed that results for dynamic and stability characteristics of partial bearing with couple stress lubrication are not available, so to validate the program for dynamic characteristics the results of K_{xx} and C_{yy} for two different values of couple stress parameter as $l^* = 0.0$ *and* 0.1, are compared for a circular bearing [36] in Fig. 5. In Fig. 6, stability characteristics of a circular bearing are compared for critical mass and threshold speed [42].

Table 1. Validation of results with published results for β = 120°, C_d=0.0 and λ = 1.0

Validation	Validation of Load characteristics ($\beta = 120^o$, C_d=0.0 *and* $\lambda = 1.0$)						
	ε= 0.1	ε = 0.2	ε = 0.3	ε = 0.4	ε = 0.5	ε = 0.6	ε = 0.7
Load by Ref. [9]	0.36	0.64	1.05	1.75	2.5	3.95	6.3
Load by Present	0.29459 8678	0.6349 21731	1.0570 34318	1.6461 69757	2.5269 19162	3.9308 78482	6.46199 5914
Validation	Validation of Pressure characteristics ($\beta = 120^o$, C_d=0.0 *and* $\lambda = 1.0$)						
	ε = 0.1	ε = 0.2	ε = 0.3	ε = 0.4	ε = 0.5	ε = 0.6	
Pressure by Ref.[9]	0.2	0.4	0.65	1.105	1.7	2.755	
Pressure by Present	0.17215 5961	0.3768 23593	0.6445 08865	1.0393 98577	1.6672 51688	2.7600 56022	

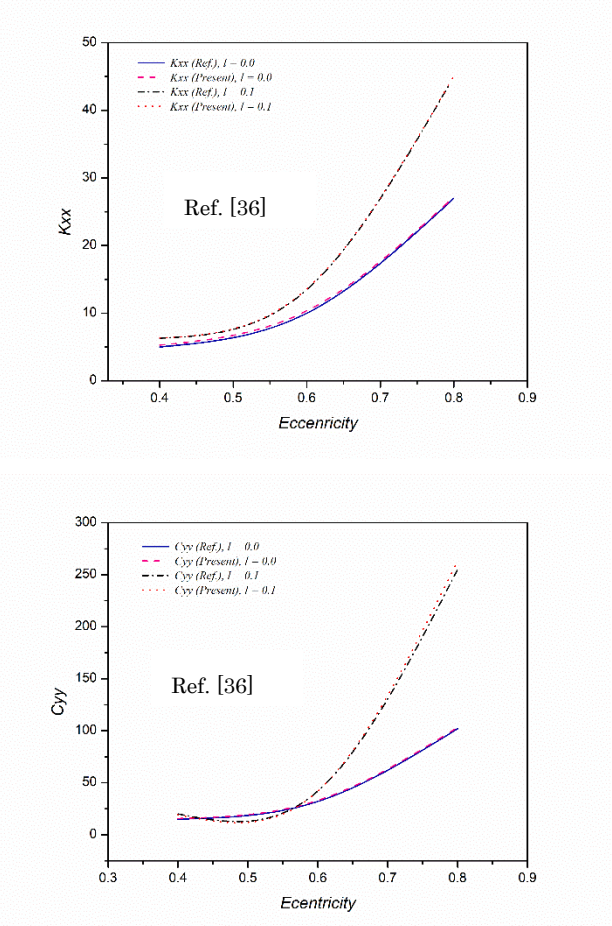

Fig. 5: Validation of dynamic characteristics (K_{xx} *and* C_{yy})

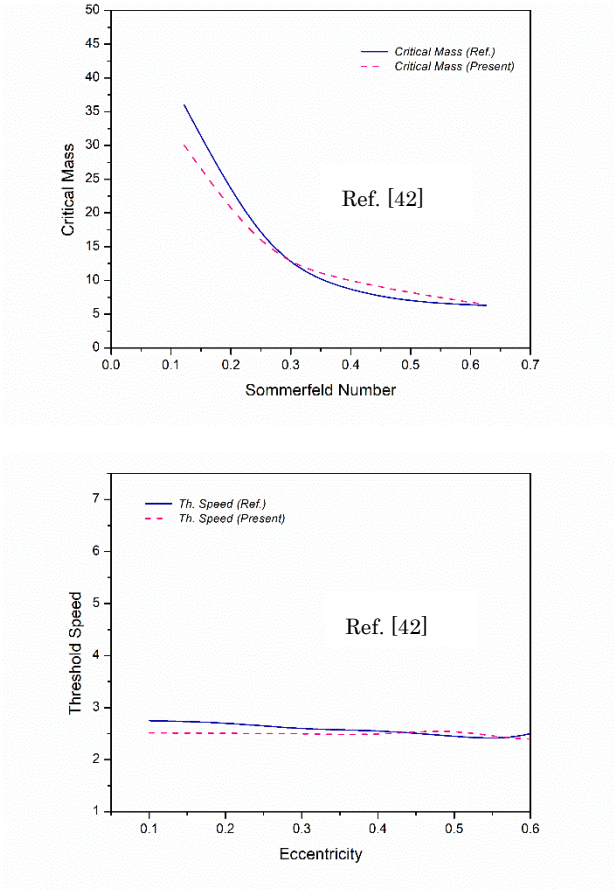

Fig. 6: Validation of stability characteristics (M_c *and* ω_{th})

On comparing, the results calculated using present program, with the available results of reference it shows a good agreement. The only difference shown here is due to the difference in approach used for solving the problem.

3.1. Static Properties

The distribution of pressure field along the bearing span in partial journal bearing towards circumferential and axial direction is illustrated by the curves shown in Fig. 4 (a) – (f). The pressure distribution for six different geometric conditions and eccentricity ratio ε = 0.5, are shown for hydrodynamic (C_d = 0.0) and elasto-hydrodynamic (C_d = 0.7) bearings.

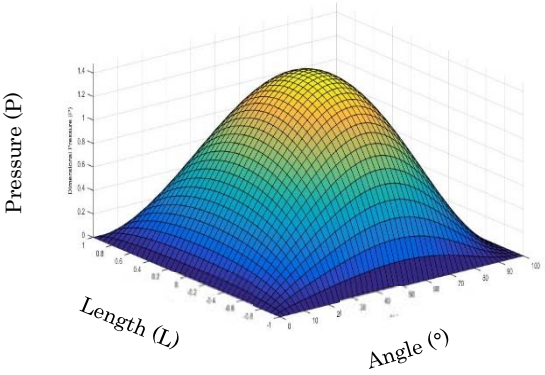

(a)

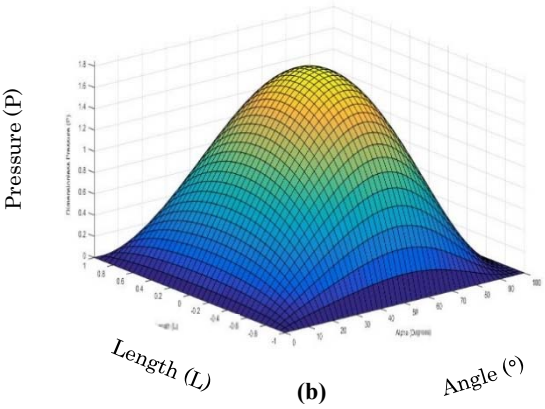

(b)

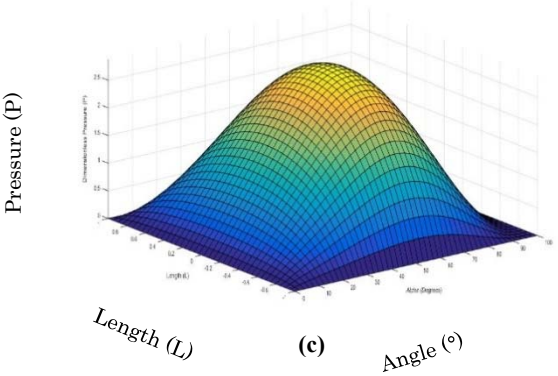

(c)

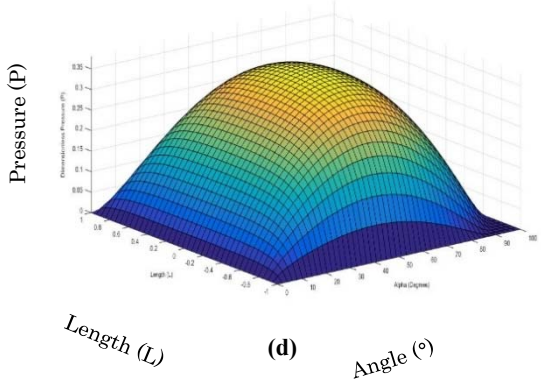

(d)

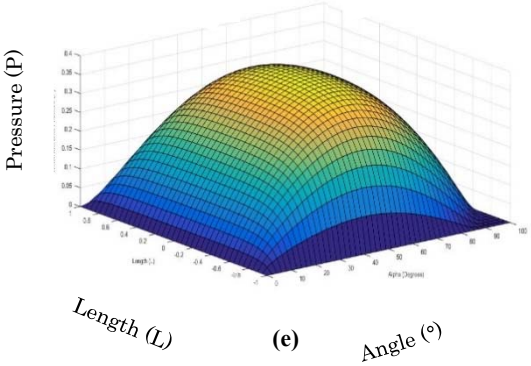

(e)

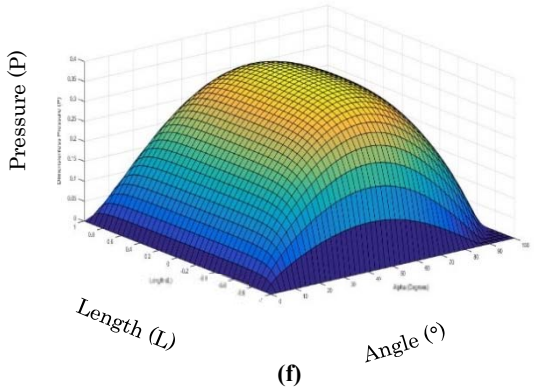

(f)

Fig. 7: Pressure distributed in discretized domain of partial journal bearing for ε = 0.5 and λ = 1.0

(a) C_d = 0.0, l* = 0.0 (b) C_d = 0.0, l* = 0.1(c) C_d = 0.0, l* = 0.2

(d) C_d = 0.7, l* = 0.0 (e) C_d = 0.7 l* = 0.1 (f) C_d = 0.7, l* = 0.2

It is observed from Fig. 7 (a) – (c) that in case of hydrodynamic bearings without flexibility in bearing liner, the pressure $\bar{p}$ increases as the value of (*CSP*) changes from 0.0 (Newtonian) to 0.1 and 0.2. In the same manner, the pressure field in partial bearings with consideration of liner deformation is enhanced for the case of (*CSP*) as 0.0 (Newtonian) to 0.1, and 0.2, as observed from Fig. 7 (d) – (f).

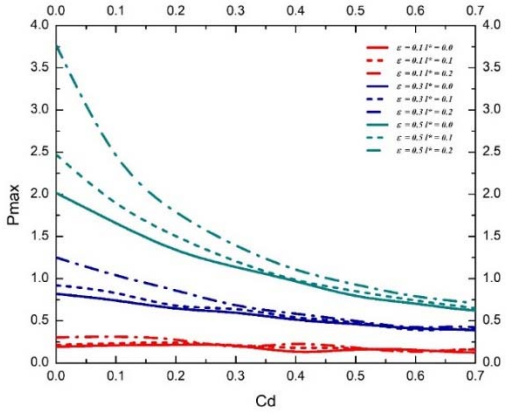

Fig. 8: Maximum pressure (P_{max}) with C_d

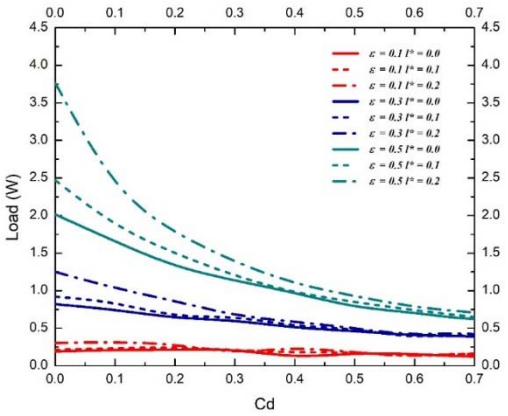

Fig. 9: Load bearing capacity ($\bar{W}$) with C_d

The change of maximum pressure, P_{max} with change in the deformation coefficient (C_d) and different values of (ε), depicted from Fig. 8, according to which the P_{max} decreases as the value of (C_d) increases from 0.0 to 0.7. It is also observed that for the value of ε = 0.1, 0.3 and 0.5, the maximum pressure increases with an increase in (ε). A considerable change in the value of P_{max} observed by using (*CSF*) as lubricant in comparison to fluid with Newtonian nature. When the flexibility of bearing liner increases for a particular eccentricity for both the Newtonian and (*CSF*) lubricant, the load capacity is reduced as shown in Fig. 6. It is clear from the graph that on increasing eccentricity ratio for any (C_d), the capacity of load bearing is increased. The result of using (*CSF*) in comparison to Newtonian fluid causes an enhancement in the capacity of load bearing for any (C_d) at any eccentricity. The load capacity is increased with an increase in the value of (*CSP*) *l** as depicted from Fig. 9.

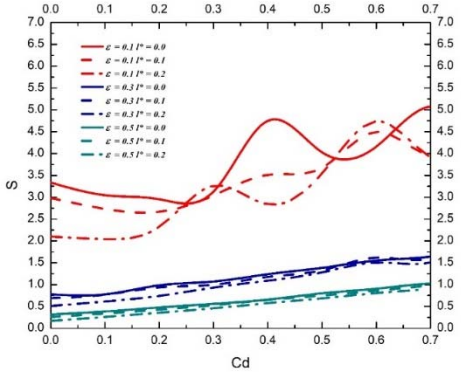

Fig. 10: Somerfeld Number (S) with C_d

The variation of Somerfeld number with flexibility (C_d), presented in Fig. 10. The parameter (S) improved with an improvement in the value of (C_d), ranging from 0.0 to 0.7, but when the medium of fluid is changed from Newtonian to non- Newtonian (i.e *CSF*) the value of Somerfield number is decreased. There is a decrease of Somerfield

number from 1.023338 in Newtonian fluid to 0.89737 in couple stress fluid, which shows a decrement of 12.597% in couple stress fluid compared to Newtonian fluid. The Somerfield number also reduced with the increase of eccentricity ratio in flexible bearing.

3.1. Dynamic Properties

When the flexibility of bearing increases it effects the pressure, as it shows a decreased trend. The increase in flexibility generates an increase in the space between surfaces of journal and bearing which effect the pressure profile in fluid film. Which in turn effects the reaction of fluid film in journal bearing system during operation. Due to a decrease in pressure and reaction in fluid film, the capacity of load bearing for the system is reduced. Fig. 11 (a), (b) shows the behavior of direct stiffness coefficient in flexible bearing with the change in eccentricity ratio and (C_d). The Direct stiffness coefficients $\overline{K}_{xx}$ and $\overline{K}_{yy}$ both increases with an increase in the (*CSP*) from $l^* = 0.0$ to 0.2. For small eccentricity i.e. ε = 0.1 both the $\overline{K}_{xx}$ and $\overline{K}_{yy}$ shows a small change in their behavior with increased (*CSP*). With an increase in (C_d) both the $\overline{K}_{xx}$ and $\overline{K}_{yy}$ seems to be almost constant and shows negligible change in their values. It shows that there is no effect or very small effect of flexibility on stiffness coefficients for small eccentricities. On increasing, the value of ε from 01 to 0.3, $\overline{K}_{xx}$ & $\overline{K}_{zz}$ both shows an enhanced increment in their values with the increase in (*CSP*), whereas a trend of decrease is shown by their graphs after increasing the (C_d) (0.1 to 0.7).

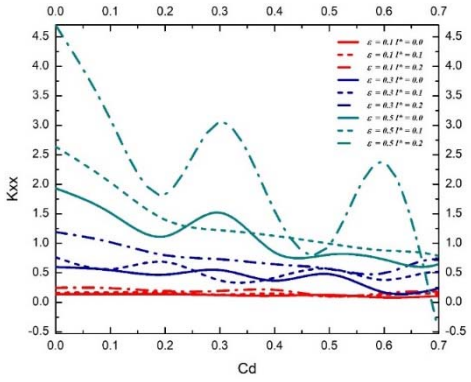

(a)

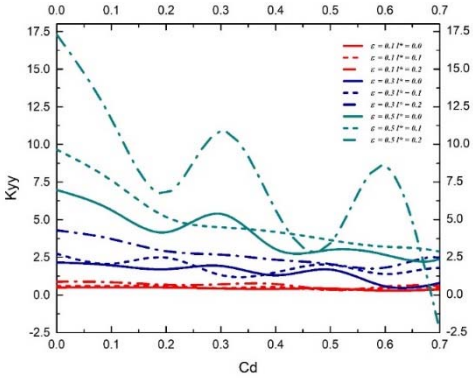

(b)

Fig. 11: Direct Coupled Stiffness ($\overline{K}_{xx}$, $\overline{K}_{yy}$) with C_d: (a) $\overline{K}_{xx}$, (b) $\overline{K}_{yy}$

The variation of $\overline{K}_{yy}$ with an increase in (C_d) for eccentricity ratio, ε = 0.5 and l^* = 0.2, shows an oscillating trend, initially between (C_d) = 0.0 - 0.2 it decreases, then increases from 0.2 - 0.3. After 0.3 - 0.5 the value of $\overline{K}_{yy}$ again decreases, whereas from 0.5 - 0.6 it is increased and from 0.6 – 0.7 it shows a decrease in its value such that at (C_d) = 0.7 it gives us a negative value. $\overline{K}_{xx}$ shows a similar trend as of $\overline{K}_{yy}$ for higher eccentricities. In case of cross stiffness coefficients it is shown by Fig. 12 (a), (b) that by increasing the value of (*CSP*) (l^* = 0.0 to 0.2) $\overline{K}_{xz}$ is going to be increased whereas $\overline{K}_{zx}$ decreases with l^* increases. When the partial arc bearing is working with using the Newtonian fluid and couple stress fluid, a change in the behavior of cross stiffness coefficient is there in the case using (CSF) in comparison with Newtonian fluid as shown by Fig. 12 (a), (b). At ε = 0.1, the effect of change in (C_d) on $\overline{K}_{xy}$ and $\overline{K}_{yx}$ shows a very small change in their behavior. Whereas at higher eccentricity ratios i.e. ε = 0.5, $\overline{K}_{yx}$ is increasing with increase in (C_d). From Fig. 9 (a) it shows that $\overline{K}_{xy}$ gives an oscillating behavior (first decreasing , then increasing and again further decreasing and then increasing) with an increase in (C_d) at higher eccentricity ratio (ε = 0.5) for l^* = 0.2. This behavior with abrupt changes with (C_d) help us to know that how the stability of the partial arc bearing system is affected at higher eccentricity ratios and higher values of *CSP* (l^* = 0.2).

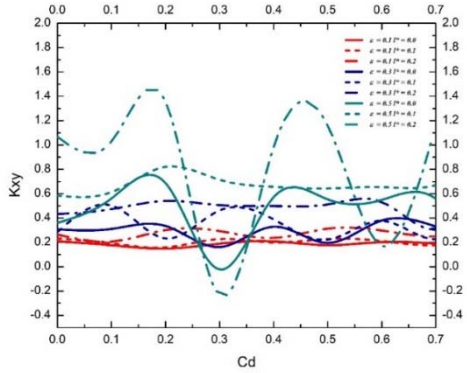

(a)

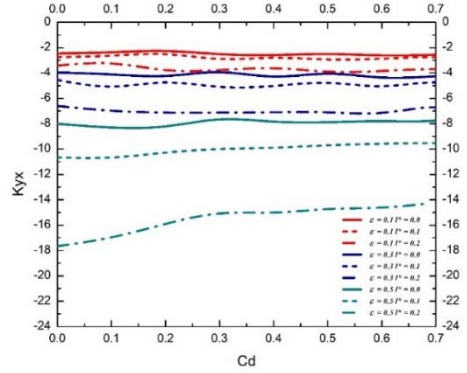

(b)

Fig. 12: Cross-Coupled Stiffness ($\bar{K}_{xy}$, $\bar{K}_{yx}$) with C_d: (a) $\bar{K}_{xy}$, (b) $\bar{K}_{yx}$

It is shown in Fig. 13 (a), (b) that how the direct damping coefficients varies with an increase in (*CSP*) (l^*) and flexibility parameter (C_d). The direct damping coefficient $\bar{C}_{xx}$ is increased with an increase in l^* and an increase in the value of eccentricity ratio. The $\bar{C}_{yy}$ also shows the same pattern of changing behavior with l^* and eccentricity ratio. The variation of direct damping coefficient $\bar{C}_{xx}$ and $\bar{C}_{yy}$ with (C_d) is found to be remains constant or very small change with an increase in (C_d) at $\varepsilon = 0.1$. On the high value of eccentricity ratio ($\varepsilon = 0.5$) both the damping coefficients (direct) ($\bar{C}_{xx}$ and $\bar{C}_{yy}$) decreases with the increase in flexibility parameter (C_d). As the load, capacity $\bar{W}$ is affected by the increase in (C_d) such that the capacity of load bearing $\bar{W}$ decreases with an increase in (C_d). Due to this pressure in the fluid film decreases and the thickness of fluid film, such that reactions are varying proportional to the $\bar{W}$, and with a decrease in fluid film reactions the pressure decreases. Therefore an increase in (C_d) give rise to a decrease in $\bar{W}$, which leads to a reduction in direct damping coefficients ($\bar{C}_{xx}$ & $\bar{C}_{yy}$) at $\varepsilon = 0.5$ and $l^* = 0.2$.

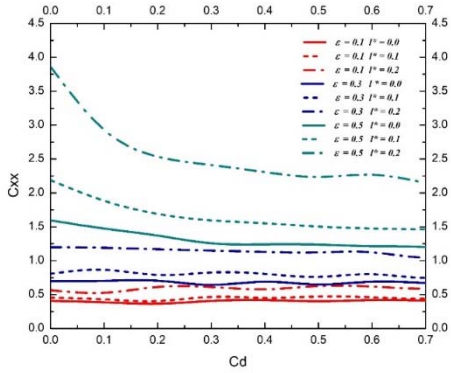

(a)

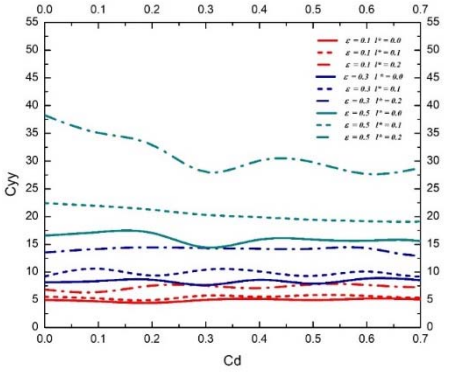

(b)

Fig. 13: Direct Coupled Damping ($\bar{C}_{xx}$, $\bar{C}_{yy}$) with C_d: (a) $\bar{C}_{xx}$, (b) $\bar{C}_{yy}$

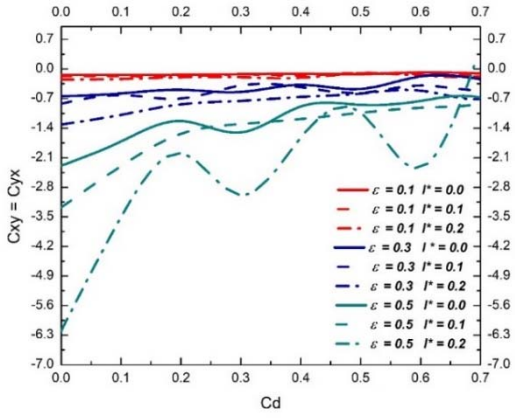

Fig. 14: Cross Coupled Damping ($\bar{C}_{xy} = \bar{C}_{yx}$) with C_d

Fig. 14 gives us the results for the variation of cross damping coefficients with l^*, (C_d), and ε. At an eccentricity ratio 0.1, $\bar{C}_{xy}$ & $\bar{C}_{yx}$ shows a very small change in their values with increasing l^*. On increasing the value of ε, the cross damping coefficient $\bar{C}_{xy}$ and $\bar{C}_{yx}$ shows an enhanced decrease in their values when increasing l^* and eccentricity ratio. The cross damping

coefficients ($\bar{C}_{xy}$ & $\bar{C}_{yx}$) improved with an increase in *(C_d)* at higher values of eccentricity ratios and (*CSP*). Fig. 14 shows that $\bar{C}_{xy}$ & $\bar{C}_{yx}$ have negative values for the entire ε and *(C_d)* with changing l^*.

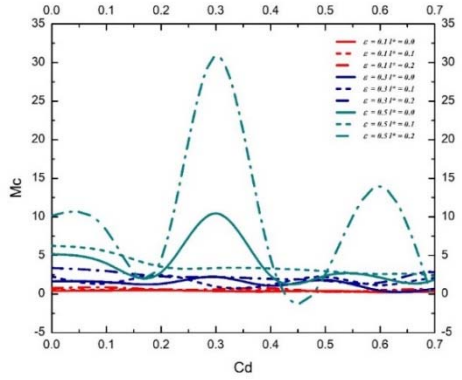

Fig. 15: Critical Mass ($\bar{M}_c$) with C_d

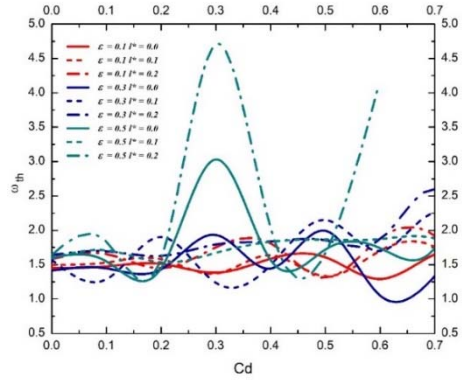

Fig. 16: Threshold Speed (ω_{th}) with C_d

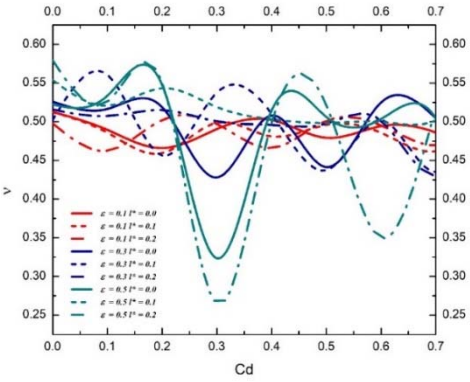

Fig. 17: Whirl Frequency (υ) with C_d

Fig. 15-17 represents stability margins in terms of critical mass ($\bar{M}_c$), threshold speed (ω_{th}) and whirl frequency *(υ)*. It is founded from Fig. 15 that critical mass ($\bar{M}_c$) is increased with an increase in the (*CSP*) (l^*), whereas it is decreased with an increase in *(C_d)*. The decrease in the value of ($\bar{M}_c$) with *(C_d)* is at a faster rate in case of higher eccentricity when ε = 0.5 and l^* = 0.2 in comparison with the Newtonian fluid. Fig. 16 gives the variation of threshold speed *(ω_{th})* with the change in l^* and *(C_d)*. The value of *(ω_{th})* is increased with an increase in l^* and the variation of *(ω_{th})* with *(C_d)* exhibits the same manner of increased behavior as observed in case of variation with l^*. The whirl frequency *(υ)* is found to be decreased with an increase in l^* and *(C_d)* both as shown in Fig. 17. Thus, it is observed from Fig. 12-14 that the stability of the partial arc bearing with flexibility is increased by using the (*CSF*) as lubricant in comparison to the fluid with Newtonian nature.

4. Conclusion

The change in the reactions of fluid film caused due to change in the fluid film extent in a bearing with partial arc with flexible liner studied here with β = 100° and a lubrication of (*CSF*). The pressure profile enhanced due to flexibility and the (*CSF*), such that the characteristics (static and dynamic) of the bearing are enhanced by using (*CSF*). The conclusions made are as follows:

1. The pressure in both the hydrodynamic and elasto-hydrodynamic bearing increases with an increase in (*CSP*) *(l^*)*.
2. The value of maximum pressure i.e. P_{max} decreases with an increase in flexibility parameter (C_d), whereas with an increase in (*CSP*) the value of P_{max} increases.
3. The capacity of load bearing ($\bar{W}$) is reduced for any value of *(ε)* with an increase in *(C_d)*. With an increase in (*CSP*) for any *(C_d)*, the ($\bar{W}$) is increased in comparison with Newtonian fluid.
4. The sommerfeld number (*S*) for the bearing is increased with an increase in *(C_d)*, whereas it is decreased with (*CSP*) in comparison with Newtonian fluid.
5. The direct stiffness ($\bar{K}_{xx}$) and ($\bar{K}_{yy}$) increases with increase in (*CSP*) for high values of eccentricity ratios. The effect of change in flexibility parameter *(C_d)* for small eccentricity ratio is very small, whereas for higher eccentricity ratios the ($\bar{K}_{xx}$) and ($\bar{K}_{yy}$) shows a trend of decrease with an increase in *(C_d)*.
6. The cross- coupled stiffness coefficients ($\bar{K}_{yx}$) is increasing with an increase in *(C_d)* whereas ($\bar{K}_{xy}$) gives an oscillating behaviour with increase in *(C_d)* at ε = 0.5 and l^* = 0.2, such the magnitude of $\bar{K}_{xz}$ is increased from 1.0678 at *(C_d)* = 0.0 to 1.157 at *(C_d)* = 0.7. The influence of change in (*CSP*) on cross stiffness is such that, $\bar{K}_{xy}$ is increased with an increase in (*CSP*) whereas $\bar{K}_{yx}$ is decreased.
7. The change in direct damping coefficients ($\bar{C}_{xx}$) and ($\bar{C}_{yy}$) with *(C_d)* is very small for small eccentricity ratios, whereas at higher eccentricity ratio i. e. ε = 0.5, both $\bar{C}_{xx}$ and $\bar{C}_{yy}$ are decreased with an increase in *(C_d)*. The cross damping coefficients ($\bar{C}_{xy}$) and ($\bar{C}_{yx}$) decreases with an increase in l^* and ε, whereas these are increasing with an increase in *(C_d)*.

8. The stability of the partial journal bearing obtained and presented by critical mass ($\bar{M}_c$), threshold speed *(ω_{th})* and whirl frequency *(ν)*. The critical mass ($\bar{M}_c$) is found to be increased with an increase in (*CSP*), whereas it is decreased with increasing *(C_d)*. The threshold speed *(ω_{th})* is improved with increase in *l** and *(C_d)* both. The whirl frequency *(ν)* is decreased with an increase in *(C_d)* and *l** both.

Thus, it is concluded that the conduct of a bearing with partial arc in terms of static and dynamic properties is enhanced by using couple stress fluid (*CSF*) as lubricant in comparison to a fluid with Newtonian nature. It is also concluded that the stability of a bearing with partial arc is improved by using the couple stress fluid (*CSF*) as lubricant in comparison to a fluid with Newtonian nature.

Acknowledgements

I am highly thankful to my co-authors Prof. Vinod Kumar and Dr. Rajiv Verma for helping me to achieve the results of this research. I am thankful to the Head, Mechanical Engineering, NIT Kurukshetra for providing me the Lab facilities for getting the results.

Nomenclature

c	Radial clearance (mm), $c = R-r$
C_d	Deformation coefficient
C_{ij}	Damping coefficient (dimensional) (Ns/mm)
$\bar{C}_{ij}$	Damping coefficient (non-dimensional), $\bar{C}_{ij} = \frac{C_{ij}c^3}{\mu_0 R_j^4}$
$\bar{C}_{xx}, \bar{C}_{yy}$	Direct damping coefficients (non-dimensional)
$\bar{C}_{xy}, \bar{C}_{yx}$	Cross damping coefficients (non-dimensional)
D	Journal Diameter (mm), $D = 2R_j$
e	Eccentricity of journal (mm)
$[F]$	Surface traction vector
h	Fluid film thickness (dimensional) (mm)
$\bar{h}$	Fluid film thickness (non-dimensional), $\bar{h} = {}^{h}/_{c}$
K_{ij}	Stiffness coefficients (dimensional) (N/mm)
$\bar{K}_{ij}$	Stiffness coefficient (non-dimensional), $K_{ij} = \frac{K_{ij}c^3}{\mu_0 R^4}$
$\bar{K}_{xx}, \bar{K}_{yy}$	Direct stiffness coefficients (non-dimensional)
$\bar{K}_{xy}, \bar{K}_{yx}$	Cross stiffness coefficients (non-dimensional)
L	Length of bearing (mm)
l	Characteristic length of additives (mm), $l = (\eta/\mu)^{1/2}$
l^*	Dimensionless couple-stress parameter, $l^* = l/c$
$\bar{M}j$	Mass of journal (Kg)
$\bar{M}_c$	Critical mass of journal (Kg)
O_b	Centre of bearing
O_j	Centre of journal
p	Pressure distribution (dimensional) (N/mm^2)
$\bar{p}$	Pressure distribution (non-dimensional), $\bar{p} = \frac{pc^2}{\mu \omega R^2}$
R_j	Radius of journal (mm)
S	Somerfield Number
t	Time (s)
W	Load bearing capacity (dimensional) (N)
$\bar{W}$	Load bearing capacity (non-dimensional), $\frac{Wc^3}{\mu \omega R^4}$
$\bar{W}_x, \bar{W}_z$	Load in x direction and z direction
X_j, Z_j	Journal centre coordinates
$\bar{z}$	Axial coordinate, $\bar{z} = {}^{Z}/_{L}$
θ	Circumferential coordinate, $\theta = X/R$
μ	Lubricant dynamic viscosity (Pa-s)
μ_0	Dynamic viscosity for reference (Pa-s)
$\bar{\mu}$	Dynamic viscosity (non-dimensional), $\bar{\mu} = {}^{\mu}/_{\mu_0} = 1$
ω_j	Rotational speed of journal (rad/s)
ω_{th}	Threshold speed (non-dimensional)
Φ	Attitude angle (^{0})
η	new material constant peculiar to *CSF*
ε	Eccentricity ratio, $\varepsilon = e/c$
λ	Aspect ratio, $\lambda = L/D$
β	Arc length of partial arc bearing
β_1	Angular position at start of partial bearing
β_2	Angular position at end of partial bearing
δ_r	Radial deformation of bearing liner

References

1) P. C. Warner, "Static and Dynamic Properties of Partial Journal Bearings," *Journal of Basic Engineering,* 247-255 (1963). doi:10.1115/1.3656569.
2) P. C. Warner, and R. J. Thoman "The Effect of the 150-Degree Partial Bearing on Rotor-Unbalance Vibration," *Journal of Basic Engineering*, 337-345 (1964). doi:10.1115/1.3653074.
3) R. J. Wernick, and C. H. T. Pan, "Static and Dynamic Characteristics of Self-Acting, Partial-Arc, Gas Journal Bearings," *Journal of Basic Engineering*, 405-413 (1964). doi:10.1115/1.3653089.

4) F. K. Orcutt, “Investigation of a Partial Arc Pad Bearing in the Superlaminar Flow Regime,” *Journal of Basic Engineering*, 145-152 (1965). doi:10.1115/1.3650491.
5) E. J. Jr. Guntur, “The Influence of Lubricant Compressibility on the Performance of 120 Degree Partial Journal Bearing,” *Journal of Lubrication Technology*, 473-481 (1967). doi:10.1115/1.3617035.
6) S. J. Dudzinsky, F. J. Young, and W. F. Hughes, “On the Load Capacity of the MHD Journal Bearing,” *Journal of Lubrication Technology*, 139-144 (1968). doi:10.1115/1.3601529.
7) F. K. Orcut and E.B. Arwas, “The Steady-State and Dynamic Characteristics of a Full Circular Bearing and a Partial Arc Bearing in the Laminar and Turbulent Flow Regimes,” *Journal of Lubrication Technology*, 143-153 (1967). doi:10.1115/1.3616932.
8) T. S. Yu and A. Z. Szevi, “Partial Journal Bearing Performance in the Laminar Regime,” *Journal of Lubrication Technology*, 94-100 (1975). doi:10.1115/1.3452541.
9) S. C. Jain, R. Sinhasan and D. V. Singh, “Elasto-hydrodynamic lubrication analysis of partial arc journal bearings,” *Tribology International*, **15** *(3)*, 161–168 (1982). doi:10.1016/0301-679X(82)90135-9.
10) M. Chandra, M. Malik and R. Sinhasan, “Gas bearings part II: Design data for centrally loaded partial arc journal bearings,” *Wear*, **89** *(2)*, 163–171 (1983). doi:10.1016/0043-1648%2883%2990241-7.
11) H. Moes, E. G. Sikkes and R. Bosma,“Mobility and Impedence Tensor Methods for Full and Partial-Arc Journal Bearings,” *Journal of Tribology*, **108**, 612-619 (1986). doi:10.1115/1.3261282.
12) R. H. Buckholz and J. F. Lin, “The Effect of Journal Bearing Misalignment on Load and Cavitation for Non-Newtonian Lubricants,” *Journal of Tribology*, **108**, 645-654 (1986). doi:10.1115/1.3261295.
13) J. F. Lin and L. Y. Wang, “Thermohydrodynamic analysis of finite-width, partial-arc journal bearings with non-Newtonian lubricants: Part II," *Tribology International*, **23** *(3)*, 211-216 (1990). doi:10.1016/0301-679X%2890%2990018.
14) H. Hashimoto and M. Mongkolwongrojn, “Adiabatic Approximate Solution for Static and Dynamic Characteristics of Turbulent Partial Journal Bearings With Surface Roughness,” *Journal of Tribology*, **116**, 672-680 (1994). doi:10.1115/1.2927315.
15) M. B. Dobrica, M. Fillon, and P. Maspeyrot, “Influence of mixed-lubrication and rough elastic-plastic contact on the performance of small fluid film bearings,” *Tribology Transaction*, **51** *(6)*, 699–717 (2008). doi:10.1080/10402000801888903.
16) M. B. Dobrica and M. Fillon, “Influence of Scratches on the Performance of a Partial Journal Bearing,” 2008. *Proc. of STLE/ASME International Joint Tribology Conference*, 1-3 (2008). doi:10.1115/IJTC2008-71170.
17) D. A. Bompos, P. G. Nikolakopoulos, C. I. Papadopoulos and L. Kaiktsis, “A Tribological Study of Partial-Arc Bearings with Egg-Shaped Surface Texture for Microturbine Applications,” *Proc. of ASME Turbo Expo 2012*, 1-10 (2012). doi:10.1115/GT2012-69383.
18) Attia Hili Molka, Bouaziz Slim, Maatar Mohamed, Fakhfakg Tahar and Haddar Mohamed, “Hydrodynamic and elastohydrodynamic studies of a cylindrical journal bearing,” *Journal of Hydrodynamics*, **22** *(2)*, 155–163 (2010). doi:10.1016/S1001-6058(09)60041.
19) K. Kohno, S. Takahakshi and K. Saki, “Elasto-hydrodynamic lubrication analysis of journal bearings with combined use of boundary elements and finite elements,” *Engineering Analysis with Boundary Elements*, **13**, 273-281 (1994). doi:10.1177/1350650116630207.
20) S. C. Jain, R. Sinhasan and D. V. Singh, “Elastohydrodynamic analysis of a cylindrical journal bearing with a flexible bearing shell,” *Wear*, **78** *(3)*, 325–335 (1982). doi:10.1016/0043-1648(82)90243-5.
21) A. A. Elsharkawy and L. H. Guedouar, “Direct and inverse solutions for elastohydrodynamic lubrication of finite porous journal bearings,” *Journal of Tribology*, **123** *(2),* 276–282 (2001). doi:10.1115/1.1308025.
22) Y. Okamoto, M. Hanahashi, and T. Katagiri, “Effects of Housing Stiffness and Bearing Dimension on Engine Bearing Performance by Elastohydrodynamic Lubrication Analysis,” *Journal of Tribology*, **122**, 697-704 (2000). doi:10.1115/1.1314604.
23) I. Nigo Arregui and C. V Azquez, “Finite element solution of a Reynolds-Koiter coupled problem for the elastic journal-bearing,” *Computer Methods in Applied Mechanics and Engineering*, **190**, 2051-2062 (2001). doi:10.1016/S0045-7825(00)00221-8.
24) Y. Changru, N. Takata, K. Thu, and T. Miyazaki “How lubricant plays a role in the heat pump system,” *EVERGREEN Joint Journal of Novel Carbon Resource Sciences & Green Asia Strategy,* **8** (1) 198–203 (2021). doi:10.5109/4372279.
25) Yanaur, Ibadurrahman, A. S. Pamitran, Gunawan, and S. Mau “Experimental investigation on the spiral pipe performance for particle-laden liquids,” *EVERGREEN Joint Journal of Novel Carbon Resource Sciences & Green Asia Strategy*, **7** (4) 580–586 (2020). doi:10.5109/4150509.
26) V. K. Stokes, “Couple Stress in Fluids,” *Physics of Fluids*, **9**, 1709–1715, (1956). doi:10.1063/1.1761925.
27) D. R. Oliver, “Load enhancement effects due to polymer thickening in a short model journal bearing,” *Journal of Non-Newtonian Fluid Mechanics*, **30**, 185–196, (1988). doi:10.1016/0377-0257(88)85024-

9.
28) H. A. Spikes, "The behaviour of lubricants in contacts : current understanding and future possibilities," *Part J: Journal of Engineering Tribology*, **208**, 3-15, (1994). doi:10.1243%2FPIME_PROC_1994_208_345_02.
29) J. R. Lin, "Squeeze film characteristics of long partial journal bearings," *Tribology International*, **30** *(1)*, 53-58 (1997). doi:10.1016/0301-679X(96)00022-9.
30) J. R. Lin, C. B. Yang and R. F. Lu., "Effects of couple stresses in the cyclic squeeze films of finite partial journal bearings," *Tribology International*, **34** *(2)*, 119–125 (2001). doi:10.5560/ZNA.2011-0009.
31) J. R. Lin, "Static and dynamic behaviours of pure squeeze films in couple stress fluid-lubricated short journal bearings," *Proc. Instn. Mech Engrs: Part J*, **211**, 29-36 (1997). doi:10.1243%2F1350650971542291.
32) S. K. Lambha, V. Kumar and R. Verma, "Elastohydrodynamic analysis of couple stress lubricated cylindrical journal bearing," *Journal of Physics: Conference Series*, **1240** *(1)*, 1-9 (2019). doi:10.1088/1742-6596/1240/1/012165.
33) N. C. Das, "A study of optimum load-bearing capacity for slider bearings lubricated with couple stress fluids in magnetic field," *Tribology International*, **31** *(7)*, 393-400 (1998). doi:10.1016/S0301-679X(98)00050-4.
34) M. Lahmar, "Elastohydrodynamic analysis of double-layered journal bearings lubricated with couple-stress fluids," *Part J: Journal of Engineering Tribology*, **219** *(2)*, 145–171 (2005). doi:10.1243%2F135065005X9835.
35) S. P. Chippa and M. Sarangi, "Elastohydrodynamically lubricated finite line contact with couple stress fluids," *Tribology International*, **67**, 11–20, (2013). doi:10.1016/j.triboint.2013.06.014.
36) P. K. Rohilla, R. Verma and S. Verma, "Performance analysis of couple stress fluid operated elastic hydrodynamic journal bearing," *Tribology Online*, **14** *(3)*, 143–154 (2019). doi:10.2474/trol.14.143.
37) R. Verma and P. Mathur, "Transient analysis of plain circular bearing with micropolar fluid," *Lect. Notes Mech. Eng.*, **12**, 143–155 (2014).
38) A. Chaudhary, A. K. Rajput, and R. Verma, "Effect of CSL on the characteristics of six-pocket hybrid irregular journal bearing," *Proc. Inst. Mech. Eng. Part J Journal of Engg. Tribology*, **235 (**3), 481–494 (2021). doi:10.1177%2F1350650120936856.
39) P. K. Rohilla, R. Verma, and S. Verma "Radial deformation analysis of couple stress fluid operated multi-lobe hydrodynamic journal bearing," *Materials Today Proc.*, xxx–xxx (2020). doi:10.2474/trol.14.143
40) S. C. Jain and R. Sinhasan "Performance of flexible shell journal bearings with variable viscosity lubricants," *Tribology International*, 331–339 (1983). doi:10.1016/0301-679X(83)90043-9
41) J. R. Lin "Linear stability analysis of rotor bearing system: couple stress fluid model," *Computers & Structures*, 801–809 (2001). doi: 10.1016/S0045-7949(00)00189-9
42) R. Sinhasan and K. C. Goyal "Transient response of a circular journal bearing lubricated with non-newtonian lubricants," *Wear*, 385–399 (1992). doi: 10.1016/0043-1648(92)90230-6
43) A. Kumar and S. K. Kakoty "Effect of couple stress parameter on steady-state and dynamic characteristics of three lobe journal bearing operating on TiO_2 nanolubricant," *Proc IMechE Part J: J Engineering Tribology*, 1–13 (2019). doi: 10.1177/1350650119866028
44) P. Khan, A. Dhanola and H. C. Garg "Elasto-hydrodynamic analysis of journal bearing operating with nanolubricants," *Proc IMechE Part J: J Engineering Tribology*, 1–12 (2020). doi: 10.1177/1350650120931979
45) M. Z. Mehrjardi "Dynamic stability analysis of non circular two lobe journal bearings with couple stress lubricant regime," *Proc IMechE Part J: J Engineering Tribology*, 1–18 (2020). doi: 10.1177/1350650120945517
46) S. Soni "Performance of finite bearing under the combined influence of turbulent and non-Newtonian lubrication," *Proc IMechE Part J: J Engineering Tribology*, 1–14 (2021). doi: 10.1177/1350650121993355